

Floquet FFLO superfluids and Majorana fermions in a shaken fermionic optical lattice

Zhen Zheng^{1,2,*}, Chunlei Qu^{1,*}, Xubo Zou², and Chuanwei Zhang^{1†}

¹*Department of Physics, The University of Texas at Dallas, Richardson, TX, 75080 USA*

²*Key Laboratory of Quantum Information, University of Science and Technology of China, Hefei, Anhui, 230026, People's Republic of China*

Fulde-Ferrell-Larkin-Ovchinnikov (FFLO) superfluids, Cooper pairings with finite momentum, and Majorana fermions (MFs), quasiparticles with non-Abelian exchange statistics, are two topics under intensive investigation in the past several decades, but unambiguous experimental evidences for them have not been found yet in any physical system. Here we show that the recent experimentally realized cold atom shaken optical lattice provides a new pathway to realize FFLO superfluids and MFs. By tuning shaken lattice parameters (shaking frequency and amplitude), various coupling between the s - and p -orbitals of the lattice (denoted as the pseudo-spins) can be generated. We show that the combination of the inverted s - and p -band dispersions, the engineered pseudo-spin coupling, and the attractive on-site atom interaction, naturally allows the observation of FFLO superfluids as well as MFs in different parameter regions. While without interaction the system is a topological insulator (TI) with edge states, the MFs in the superfluid may be found to be in the conduction or valence band, distinguished from previous TI-based schemes that utilize edge states inside the band gap.

Optical lattices for ultra-cold atoms provide a generic platform for quantum simulation of various condensed matter phenomena because of their precise control of the system parameters and the lack of disorder [1]. In a static optical lattice, the Bloch bands are well separated by large energy gaps and usually only one band plays a dominate role in the static and dynamical properties of ultra-cold atoms [2–4]. Current optical lattice study has mainly focused on the lowest s -orbital band, but higher-orbital (e.g., p -orbital band, etc.) physics has also been investigated extensively in both theory [5–8] and experiment [9, 10] in the past decade. Recently, the experimentally realized shaken optical lattices opens a completely new avenue for studying the physics originating from the coupling between different orbital bands induced by the lattice shaking [11]. It was shown in experiment that the hybridization of s -band and p -band of a Bose-Einstein condensate (BEC) in a shaken lattice can cause a change of the energy dispersion from a parabolic to a double well structure, yielding a paramagnetic to ferromagnetic phase transition [11–13]. More generally, by varying the shaking parameters, various coupling between different Bloch bands can be engineered to implement artificial gauge fields for cold atoms, yielding exciting new exotic physics [14, 15], such as the recent experimental observation of topological Haldane model and the associated anomalous Hall effect [16].

In this paper, we investigate new superfluid physics emerged from the coupling between the lowest two Bloch bands (s - and p -bands) in a shaken fermionic optical lattice. The s - and p -orbitals are denoted as two pseudo-spins, whose energy dispersions are inverted, in contrast to the same dispersion for usual spins. We show that such inverted band dispersions, together with attractive on-site interaction between atoms on s - and p -bands, provide a natural way to realize the long-sought Fulde-

Ferrell-Larkin-Ovchinnikov (FFLO) superfluids [17, 18]. FFLO states, first proposed in 1960s to describe the finite momentum Cooper pairings with a large Zeeman field, are a central concept for understanding many exotic phenomena in different physics branches. However, unambiguous experimental signature of FFLO states is still lacking for any physical system. Because of the inverted band dispersion, the FFLO state becomes the natural ground state of the system even without an explicit external Zeeman field.

When the shaking frequency and amplitude are tuned to certain regime, the coupling between two pseudo-spins may depend on the lattice quasi-momentum, analogous to the artificial spin-orbit coupling (SOC) [19–23]. Without interaction, the system behaves like a topological insulator (TI) [24, 25] and supports topological edge states. We show that there is a quantum phase transition from FFLO to BCS superfluids with increasing SOC. In a large parameter regime, the BCS superfluid is topological and supports Majorana fermions (MFs) which are localized at the lattice boundaries [26, 27]. MFs are quasiparticles that are their own antiparticles and possess non-Abelian exchange statistics, a crucial element for topological quantum computation. More interestingly, the topological BCS superfluids and MFs may utilize the conduction or valence bands of such a TI, instead of the edge states inside the band gap that are commonly used in previous TI-based schemes for MFs [28].

Model Hamiltonian of the shaken lattice: We first consider a degenerate spinless Fermi gas trapped in a three dimensional (3D) optical lattice. The system can be easily reduced to a quasi-2D or quasi-1D optical lattice by raising the lattice potential depths along the y and z directions, allowing only small transverse tunneling. The shaking of the lattice is along the x direction and the shaking amplitude is ramped up slowly to reach

a constant [11], yielding a periodically modulating lattice potential

$$V(x, y, t) = V_x \cos^2(k_L x + f \cos(\omega t)) + V_y \cos^2(k_L y) + V_z \cos^2(k_L z), \quad (1)$$

where V_i ($i = x, y, z$) are the lattice depths, $k_L = \pi/a$, a is the lattice spacing that is set as the length unit. f and ω are the shaking amplitude and frequency, respectively. The energy dispersions of the static Bloch bands can be shifted by $n\hbar\omega$ (n is an arbitrary integer) due to the shaking, forming the new Floquet bands. The shaking also couples two close Floquet or static bands, leading to gaps in the energy spectrum, as illustrated in Fig. 1. We focus on the lowest s - and p -bands and ignore all other higher bands for simplicity. Because the shaking is along the x direction, only the p_x -band can be coupled with the s -band and atoms stay at the s -band along the other two directions. When ω is tuned close to the band gap (Γ) of the static lattices, i.e., $\hbar\omega \sim \Gamma$, the s -orbital state can absorb an energy of $\hbar\omega$ and couple with the p_x -orbital state, similar as the Rabi oscillation between two spin states. Such “one-photon process” coupling strength is denoted by Ω , which can be approximated as a constant [29]. If we tune $\hbar\omega \sim \Gamma/2$, the s -orbital band is shifted upward by two photon energy $2\hbar\omega$ to couple with the p_x -band. In this “two-photon process”, by properly tuning the frequency and amplitude of the shaking, the dominate coupling is between the nearest neighboring sites between s - and p_x -orbital states that simulates a SOC [29].

In the basis of $(\psi_s(\mathbf{k}), \psi_{p_x}(\mathbf{k}))^T$, the single-particle Hamiltonian in momentum space reads

$$\mathcal{H}_0 = \begin{pmatrix} \epsilon_s(\mathbf{k}) + h & \Omega + \alpha \sin(k_x a) \\ \Omega + \alpha \sin(k_x a) & \epsilon_p(\mathbf{k}) - h \end{pmatrix} \quad (2)$$

under the tight-binding approximation. Here $\epsilon_s(\mathbf{k}) = -t_s \cos(k_x a) - t_s^\perp [\cos(k_y a) + \cos(k_z a)] - \mu$ and $\epsilon_p(\mathbf{k}) = t_p \cos(k_x a) - t_s^\perp [\cos(k_y a) + \cos(k_z a)] - \mu$, where t_s and t_p are the nearest neighbor tunneling amplitudes for an atom in s -orbital and p -orbital states along the x direction, and t_s^\perp is the tunneling amplitudes along the y and z directions. Ω is the momentum-independent coupling strength of the two orbital states which dominates in the one-photon process, α is the effective SOC strength which dominates in the two-photon process. μ is the chemical potential, h is the off-resonance detuning determined by the difference of the shaking frequency and the band gap. Fig. 1 illustrates the one-photon and two-photon processes and the corresponding band structures. With a finite coupling Ω or $\alpha \sin(k_x a)$, two bands are hybridized around the crossing points, and thus yield an energy gap. Note that for a 1D system with $t_s^\perp = 0$ and $t_p = t_s$, this non-interacting Hamiltonian breaks the time reversal symmetry but preserves a chiral symmetry $\sigma_y \mathcal{H}_0(k_x) \sigma_y = -\mathcal{H}_0(k_x)$, which realizes an AIII class

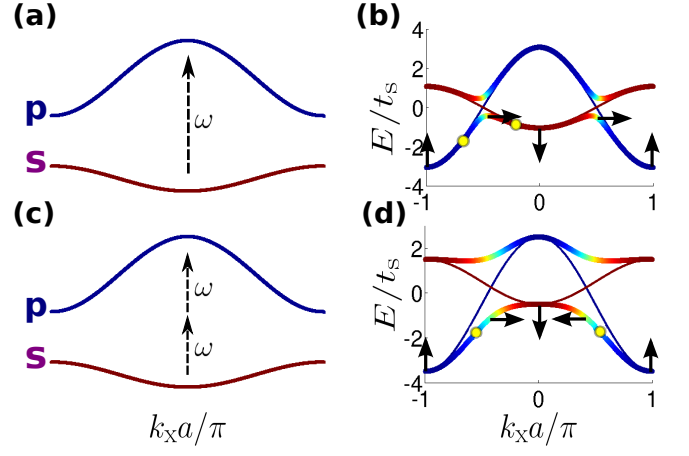


FIG. 1: **Single-particle band structure for $t_p = 3t_s$.** (a) Illustration of one-photon coupling process of the two Bloch bands. (b) Band structure of shaken lattice with finite one-photon coupling $\Omega = 0.3t_s$. (c) Illustration of the two-photon coupling process. (d) Band structure of shaken lattice with finite two-photon coupling $\alpha = 1.0t_s$ and Zeeman field $h = 0.3t_s$. To show how the coupling of two Bloch bands opens an energy gap, we also plot the band dispersion without coupling by the thin lines in (b,d). The colors in (b,d) represent the spin compositions of each momentum state and the arrows represent the spin rotations along one of the hybrid band. The yellow filled circles denote the preferred Cooper pairings.

TI characterized by a \mathbb{Z} topological invariant [30, 31]. In the topological phase, there are in-gap topological states on the boundaries of the system [32–34]. When $t_p \neq t_s$, there will be an additional kinetic energy term, which does not change the phase transition and topological properties of the system [35, 36].

We consider on-site attractive interaction between atoms on different orbital bands (see Discussion section and Supplementary Information for more discussions). Such density-density interaction is not modified by the shaking. In the momentum space, the interaction Hamiltonian can be written as $\mathcal{H}_I = -U \sum \psi_s^\dagger(\mathbf{k}_1) \psi_{p_x}^\dagger(\mathbf{k}_2) \psi_{p_x}(\mathbf{k}_3) \psi_s(\mathbf{k}_4)$, where $\mathbf{k}_1 + \mathbf{k}_2 = \mathbf{k}_3 + \mathbf{k}_4$ due to the momentum conservation in the two-body scattering processes, $U > 0$ is the interaction strength.

As the first step approach for a qualitative understanding of the interacting Fermi gas in a shaken optical lattice, we consider the mean-field approximation and assume a single-plane-wave FF-type order parameter, i.e., $\Delta = U \langle \psi_{p_x}(\frac{\mathbf{Q}}{2} - \mathbf{k}) \psi_s(\frac{\mathbf{Q}}{2} + \mathbf{k}) \rangle$, where $\mathbf{Q} = (Q, 0, 0)$ is the FF vector along the x direction. $\mathbf{Q} = 0$ corresponds to a conventional BCS superfluid. The dynamics of the system is governed by the Bogliubov-de Gennes (BdG) Hamiltonian,

$$\mathcal{H}_{\text{BdG}}(\mathbf{k}) = \begin{pmatrix} \mathcal{H}_0(\frac{\mathbf{Q}}{2} + \mathbf{k}) & \Delta \\ \Delta^* & -\sigma_y \mathcal{H}_0^*(\frac{\mathbf{Q}}{2} - \mathbf{k}) \sigma_y \end{pmatrix}, \quad (3)$$

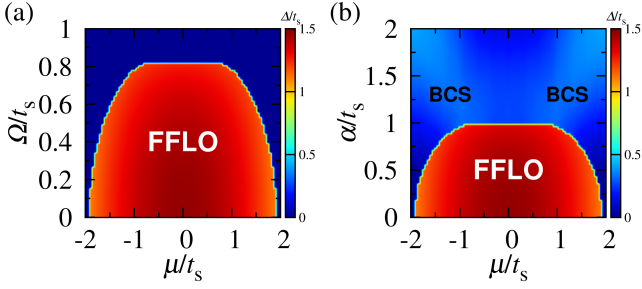


FIG. 2: **Phase diagram of a 3D shaken optical lattice with (a) one-photon coupling Ω or (b) two-photon coupling α .** The color describes the magnitude of the order parameter Δ in unit of t_s . FFLO denotes the superfluid with a finite center of mass momentum along the shaking direction $Q_x = \pm\pi$, BCS stands for the BCS superfluids with $\mathbf{Q} = \mathbf{0}$. Other parameters $U = 4.0t_s$, $h = 0.0$, $t_p = 3t_s$, $t_s^\perp = t_s$.

in the Nambu-Gorkov spinor basis $[\psi_s(\frac{\mathbf{Q}}{2} + \mathbf{k}), \psi_{p_x}(\frac{\mathbf{Q}}{2} + \mathbf{k}), \psi_{p_x}^\dagger(\frac{\mathbf{Q}}{2} - \mathbf{k}), -\psi_s^\dagger(\frac{\mathbf{Q}}{2} - \mathbf{k})]^T$. The gap and momentum equations are solved by minimizing the thermodynamic potential to obtain Δ and Q (see Methods), through which we determine different phases. When $\Delta \neq 0$ and $Q \neq 0$, the system is in a FFLO phase. When $\Delta \neq 0$, $Q = 0$, the system is in a BCS phase. Otherwise, the system is a normal gas or a band insulator.

Phase diagrams in 3D lattices: In Fig. 2 we plot the phase diagrams for resonant one-photon (Fig. 2a) and two-photon processes (Fig. 2b) with $t_p = 3t_s$, $t_s^\perp = t_s$. The phase diagram is similar for quasi-2D and quasi-1D systems with $t_s^\perp \rightarrow 0$. The system favors FFLO states in a large parameter regime with a finite momentum along the shaking direction $Q_x = \pm\pi$. Here the FFLO pairing originates from the intrinsic band dispersion inversion between s - and p_x -bands, which suppresses the conventional BCS pairing. This can be further understood through a coordinate transformation (see Methods) $k'_x \rightarrow k'_x \pm \pi$ for the p_x -band dispersion to remove the band inversion. In the system without the band inversion, we expect a conventional BCS superfluids between k_x and $-k_x$, leading to $k'_x \pm \pi = -k_x$. Therefore the preferred pairings in the shaken lattice are between two spins with momenta of k_x and $k'_x = \pm\pi - k_x$, and the FFLO momentum is $Q_x = \pm\pi$. The analysis still applies in the presence of SOC and Zeeman fields.

For a large Ω , the gap between two hybrid bands is very large, thus a band insulator phase appears near the half filling. Each of the hybrid band polarizes to one spin state for a large Ω , leading to vanishing Cooper pairing. In the presence of small SOC $\alpha \sin(k_x a)$, the system still favors the FFLO superfluid. However, the SOC $\alpha \sin(k_x a)$ leads to different wavefunctions at k_x and $-k_x$, making it possible to have the BCS pairing, as observed in Fig. 2b for a large SOC.

Topological phase and MFs in 1D lattices: Hereafter we focus on possible topological phases induced

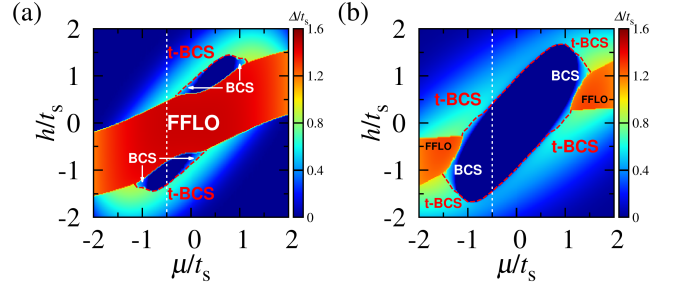


FIG. 3: **Effect of the Zeeman field on the phase diagram of the 1D shaken optical lattice with a two-photon coupling.** (a) $\alpha = 0.7t_s$; (b) $\alpha = 1.4t_s$. t-BCS represents the topological BCS superfluids. The red dashed lines are the boundary between BCS/insulator and t-BCS superfluids. $U = 4.0t_s$, $t_p = 3t_s$, $\Omega = 0.0$.

by the SOC. It is well known that there is no topological phases in a 3D system with such 1D SOC. To reach the topological phase that may support topological excitations such as MFs, we need to consider a quasi-1D system with small or vanishing transverse tunneling t_s^\perp . We first present the results for $t_s^\perp = 0$ for simplicity, and will discuss how a small t_s^\perp modifies the phase diagram and the topological phases later. In Fig. 3, we plot the phase diagrams in the presence of a Zeeman field h for two different SOC strengths, where a new phase, topological BCS (t-BCS) superfluids that host MFs, emerges in a large parameter regime. The transition from BCS to t-BCS is characterized by the bulk quasiparticle excitation spectrum closing and reopening at $k_x = 0$ (and $k_x = \pm\pi$) and can be understood from the symmetry of the BdG Hamiltonian. The BdG Hamiltonian (3) satisfies the particle-hole symmetry $\Xi \mathcal{H}_{\text{BdG}}(k_x) \Xi^{-1} = -\mathcal{H}_{\text{BdG}}(-k_x)$, where $\Xi = \Lambda \mathcal{K}$, $\Lambda = \sigma_x \tau_z$ and \mathcal{K} is the complex conjugate operator. For a BCS superfluid ($Q_x = 0$), it also respects a time-reversal-like symmetry $\mathcal{T} \mathcal{H}_{\text{BdG}}(k_x) \mathcal{T}^{-1} = \mathcal{H}_{\text{BdG}}(-k_x)$ if $t_p = t_s$, where $\mathcal{T} = \sigma_z \tau_0 \mathcal{K}$. This topological BCS superfluid belongs to the BDI symmetry class characterized by a \mathbb{Z} invariant and MFs can be found at the boundary of the superfluids [30, 31, 37]. For $t_p \neq t_s$, it belongs to the more generalized D symmetry class characterized by a \mathbb{Z}_2 invariant. The topological BCS phase region can be determined by the Pfaffian sign of the skew matrix $\Gamma(k_x) = H_{\text{BdG}}(k_x) \Lambda$ yielding

$$\text{sign}[\text{Pf}(\Gamma(0)) \times \text{Pf}(\Gamma(\pi))] = -1, \quad (4)$$

which has an explicit form

$$[(t_+ - h)^2 - \Delta^2 - (\mu + t_-)^2][(t_+ + h)^2 - \Delta^2 - (\mu - t_-)^2] < 0 \quad (5)$$

where $t_+ = (t_s + t_p)/2$, $t_- = (t_s - t_p)/2$.

Because $t_p \neq t_s$, the phase diagrams are not symmetric about $h = 0$ or $\mu = 0$ as shown in Fig. 3. However, the system is symmetric with the transformation

$h \rightarrow -h$ and $\mu \rightarrow -\mu$. This is in stark contrast to conventional systems (two pseudo-spins both in s -bands), where the phase diagrams are symmetric with respect to either $h = 0$ or $\mu = 0$ and the Zeeman field must be larger than a critical value for the appearance of t-BCS phase. Furthermore, when the inversion symmetry of the hybrid band structure is broken, it is also possible to realize the topological FFLO superfluids in the shaken optical lattice [38–41].

From Fig.3, we see the FFLO superfluid dominates for small SOC and the region of t-BCS superfluids does not change much when the strength of SOC is increased. There exists an insulator block with $\Delta = 0$ near $\mu = 0$ surrounded by the superfluid phase in Fig. 3b. Note that without the interaction, the single particle Hamiltonian \mathcal{H}_0 (with $t_s^\perp = 0$) already possesses some topological properties in the presence of the SOC. In this insulator phase, a pair of sub-gap states may appear on the system boundaries [35]. With the interaction tuned on in Fig.3(a,b), the system evolves into a topological superfluids with finite BCS order parameters. The original edge states of the topological insulator are now replaced with the zero energy Majorana boundary states [32] when the chemical potential is in the band gap, similar as previous TI based MF scheme using edge states. More interestingly, when the chemical potential cuts only one of the conduction or valance bands, we find the coexistence of the edge states from the topological insulator and the zero energy Majorana edge states from the topological superconductor.

For MFs, we can consider 1D atom tubes generated by optical lattices in a 3D system with weak tunnelings along the transverse directions. The weak transverse tunneling can strongly suppress the quantum fluctuations along the 1D tubes, similar as that in high temperature cuprate superconductors. Consider a periodic boundary condition along the transverse directions, the weak tunneling simply shifts the chemical potential of the 1D gas at most by $4t_\perp$ in Eq. (5). As long as the shifted chemical potential still stays inside the topological BCS region, we expect the MFs exist along the tube edges. Similar issue for MFs has been widely discussed in spin-orbit coupled quantum wires (nanowire or cold atom tube arrays) and our calculations show that the same conclusion still holds for the shaken optical lattices.

Quantum phase transition and Majorana fermions in real space: The above momentum space analysis is further confirmed by self-consistently solving the BdG Hamiltonian in the real space. In Fig. 4(a,b) we plot the average value of the order parameter Δ and the lowest two quasi-particle excitation energies E_1 and E_2 as a function of the Zeeman field h for (a) $\alpha = 0.7t_s$ and for (b) $\alpha = 1.4t_s$. In consistent with the white dashed lines in Fig. 3, there is a phase transition from FFLO superfluids to topological BCS superfluids at $h \approx 0.48t_s$ for small SOC in (a) and from insulator phase to trivial

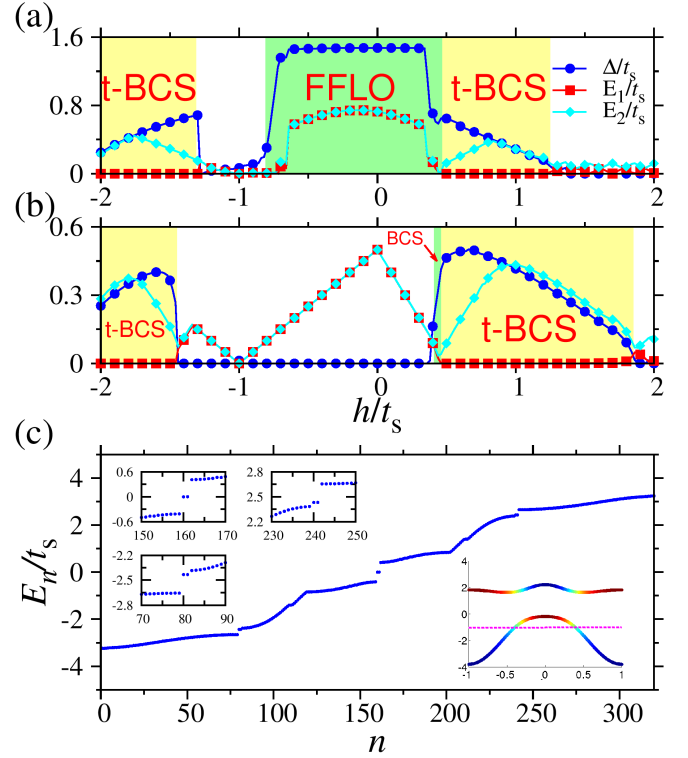


FIG. 4: **Majorana fermions in a shaken optical lattice.** (a, b) The order parameter Δ (Blue circles) and the lowest two quasi-particle excitation energies E_1 (red squares), E_2 (cyan diamonds) as a function of Zeeman field h by self-consistently solving the real space BdG equation with open boundary condition for $\alpha = 0.7t_s$ (a) and $\alpha = 1.4t_s$ (b). We have labeled the phase region for FFLO superfluids and the topological BCS superfluids with colors. Other unlabeled regions correspond to either normal gas or insulator phase. In both figures $\mu = -0.5t_s$, $U = 4.0t_s$, $\Omega = 0.0$, $t_p = 3t_s$. (c) Plot of the BdG quasi-particle excitation energies for $\alpha = 1.4t_s$, $\mu = -0.7t_s$, $h = 0.8t_s$. There are three pairs of sub-gap states all localized on the boundaries.

BEC superfluids and then to a topological BCS superfluids at $h \approx 0.45t_s$ for large SOC in (b). The momentum of FFLO Cooper pairs in real space is either FF or LO types, both have the same ground state energies as that in momentum space. In the topological phase, the zero energy Majorana fermions are protected by a finite mini-gap E_2 . In Fig. 4(c) we plot of the BdG quasi-particle excitation energies for $\mu = -0.7t_s$, $h = 0.8t_s$, $\alpha = 1.4t_s$. The inset shows the quasi-particle excitation spectrum with zero energy degenerate MF states and the single particle band structure where the chemical potential cuts a single conduction band. The zero energy Majorana fermion modes are localized on the system boundaries. Interestingly for $\mu \neq 0$ and when the chemical potential cuts either of the two bands, we may find another one pairs of sub-gap edge states with finite energies which are induced by the topological insulator. The coexistence of the reminiscent edge states from topological insulator and the MFs edge

states from topological superconductor may lead to many interesting transport properties in this system.

Discussion

For a spinless Fermi gas, the s -wave scattering interactions between same orbital states are usually prohibited by the Pauli exclusion principle, and the interactions between different orbital states are usually very small. However, the strong on-site attractive interactions can still be engineered using different methods (see more detailed discussion in Supplementary Information):

a) Bosons-mediated interactions in Bose-Fermi mixtures [42, 43], where the induced interaction between fermions by bosons can be written as screened Coulomb interaction $U_{ind}(r) = -\frac{m_B n_B U_{BF}^2}{\pi \hbar^2} \frac{\exp(-\sqrt{2}r/\xi)}{r}$. Here m_B and n_B are the mass and density of the bosons, $\xi = \sqrt{\hbar^2/2m_B n_B U_{BB}}$ is the healing length for the bosons, and U_{BF} and U_{BB} are the Bose-Fermi and Bose-Bose scattering interaction strengths that can be tuned using Feshbach resonance;

b) Dipole-dipole interaction between dipolar atoms [44]: when the dipoles are aligned along the 1D direction (i.e., head to head), the dipole interaction between atoms ($\sim 1/r^3$) is attractive. Both the screened Coulomb interaction in Bose-Fermi mixture and the long rang dipole interaction can lead to attractive on-site interaction between atoms with different orbital states at the same lattice site. For the dipolar atoms, the on-site interaction can be tuned by the lattice confinement along the transverse directions.

c) Through the interaction between the atom in the p -orbital with another s -orbital atom with different hyperfine state or different specie, where the interaction can also be tuned by Feshbach resonance. In this case, the optical lattice should be spin-dependent or species dependent so that the s -orbital of the atom does not couple to the p -orbital for the same specie. The alkali-earth or heavy alkali atoms can be used to avoid heating from spontaneous emission. For different species (i.e., Fermi-Fermi mixtures), far detuning lasers can be used without any significant heating. In this system, the s -orbital of the original atoms are assumed to be fully filled. Therefore even they interact with the additional atoms, they do not generate superfluid order. Our calculations show that FFLO states can also be generated in a certain parameter region.

Acknowledgement We thank Yong Xu, Chris Hamner and Peter Engels for helpful discussions. C. Qu and C. Zhang are supported by ARO (W911NF-12-1-0334) and AFOSR (FA9550-11-1-0313). Z.Z. and X.Z. are supported by National Natural Science Foundation of China (Grant No. 11074244 and Grant No. 11274295), and National 973 Fundamental Research Program (2011cba00200).

* These authors contributed equally to this work

† chuanwei.zhang@utdallas.edu

- [1] Bloch, I., Dalibard, J. & Nascimbene, S. Quantum simulations with ultracold quantum gases. *Nature Physics* **8**, 267-276 (2012).
- [2] Jaksch, D., Bruder, C., Cirac, J. I., Gardiner, C. W. & Zoller, P. Cold bosonic atoms in optical lattices. *Phys. Rev. Lett.* **81**, 3108-3111 (1998).
- [3] Bloch, I., Dalibard, J. & Zwerger, W. Many-body physics with ultracold gases. *Rev. Mod. Phys.* **80**, 885 (2008).
- [4] Greiner, M., Mandel, O., Esslinger, T., Hänsch, T.W. & Bloch, I. Quantum phase transition from a superfluid to a Mott insulator in a gas of ultracold atoms. *Nature* **415**, 39-44 (2002).
- [5] Liu, W. & Wu, C. Atomic matter of nonzero-momentum Bose-Einstein condensation and orbital current order. *Phys. Rev. A* **74**, 013607 (2006).
- [6] Wu, C. Orbital ordering and frustration of p -band Mott insulator. *Phys. Rev. Lett.* **100**, 200406 (2008).
- [7] Zhang, M. Hung, H.-h, Zhang, C. & Wu, C. Quantum anomalous Hall states in the p -orbital honeycomb optical lattices. *Phys. Rev. A* **83**, 023615 (2011).
- [8] Xu, Y., Chen, Z., Xiong, H., Liu, W. V. & Wu, B. Stability of p -orbital Bose-Einstein condensates in optical checkerboard and square lattices. *Phys. Rev. A* **87**, 013635 (2013).
- [9] Wirth, G., Ölschläger, M. & Hemmerich, A. Evidence for orbital superfluidity in the P -band of a bipartite optical square lattice. *Nature Physics* **7**, 147-153 (2011).
- [10] Soltan-Panahi, P., Lühmann, D., Struck, J., Windpassinger, P. & Sengstock, K. Quantum phase transition to unconventional multi-orbital superfluidity in optical lattices. *Nature Physics* **8**, 71-75 (2012).
- [11] Parker, C. V., Ha, L.-C. & Chin, C. Direct observation of effective ferromagnetic domains of cold atoms in a shaken optical lattice. *Nature Physics* **9**, 769 (2013).
- [12] Zheng, W., Liu, B., Miao, J., Chin, C. & Zhai, H. Strongly interaction effects in a superfluid ising quantum phase transition. Preprint at <http://arxiv.org/abs/1402.4569> (2014).
- [13] Choudhury, S. & Mueller, J. E. Stability of a Floquet Bose-Einstein condensate in a one-dimensional optical lattice. *Phys. Rev. A* **90**, 013621 (2014).
- [14] Lim, L.-K, Smith, C. M. & Hemmerich, A. Staggered-vortex superfluid of ultracold bosons in an optical lattice. *Phys. Rev. Lett.* **100**, 130402 (2008).
- [15] Hauke, P. *et al.* Non-Abelian gauge fields and topological insulators in shaken optical lattices. *Phys. Rev. Lett.* **109**, 145301 (2012).
- [16] Jotzu, G. *et al.* Experimental realization of the topological Haldane model. Preprint at <http://arxiv.org/abs/1406.7874> (2014).
- [17] Fulde, P. & Ferrell, R. A. Superconductivity in a strong spin-exchange field. *Phys. Rev.* **135**, 550 (1964).
- [18] Larkin, A. I. & Ovchinnikov, Y. N. Nonuniform state of superconductors. *Zh. Eksp. Teor. Fiz.* **47**, 1136 (1964).
- [19] Lin, Y.-J., Garcia, K. J. & Spielman, I. B. Spin-orbit-coupled Bose-Einstein condensates. *Nature* **471**, 83-86 (2011).
- [20] Zhang, J.-Y. *et al.* Collective dipole oscillation of a spin-orbit coupled Bose-Einstein condensate. *Phys. Rev. Lett.*

- 109, 115301 (2012).
- [21] Qu, C., Hammer, C., Gong, M., Zhang, C. & Engels, P. Observation of Zitterbewegung in a spin-orbit coupled Bose-Einstein condensate. *Phys. Rev. A* **88**, 021604(R) (2013).
- [22] Wang, P. *et al.* Spin-orbit coupled degenerate Fermi gases. *Phys. Rev. Lett.* **109**, 095301 (2012).
- [23] Cheuk, L. W. *et al.* Spin-Injection spectroscopy of a spin-orbit coupled Fermi gas. *Phys. Rev. Lett.* **109**, 095302 (2012).
- [24] Hasan, M. Z. & Kane, C. L. Topological insulators. *Rev. Mod. Phys.* **82** 3045 (2010).
- [25] Qi, X. L. & Zhang, S. C. Topological insulator and superconductor. *Rev. Mod. Phys.* **83** 1057 (2011).
- [26] Zhang, C., Tewari, S., Lutchyn, R. M. & Das Sarma, S. $p_x + ip_y$ superfluid from s -wave interactions of Fermionic cold atoms. *Phys. Rev. Lett.* **101**, 160401 (2008).
- [27] Sato, M., Takahashi, Y. & Fujimoto, S. Non-abelian topological order in s -wave superfluids of ultracold Fermionic atoms. *Phys. Rev. Lett.* **103**, 020401 (2009).
- [28] Fu, L. & Kane, C. L. Superconducting proximity effect and Majorana fermions at the surface of a topological insulator. *Phys. Rev. Lett.* **100**, 096407 (2008).
- [29] Zhang, S. & Zhou, Q. Shaping topological properties of the band structures in a shaken optical lattice. Preprint at <http://arXiv.org/abs/1403.0210> (2014).
- [30] Schnyder, A., Ryu, S., Furusaki, A. & Ludwig, A. W. W. Classification of topological insulators and superconductors in three spatial dimensions. *Phys. Rev. B* **78**, 195125 (2008).
- [31] Kitaev, A. Periodic table for topological insulators and superconductors. *AIP Conf. Proc.* **1134**, 22-30 (2009).
- [32] He, J. *et al.* Correlated spin currents generated by resonant-crossed Andreev reflections in topological superconductors. *Nat. Commun.* **5**:3232 (2014).
- [33] Liu, X.-J., Liu, Z.-X. & Cheng, M. Manipulating topological edge spins in one-dimensional optical lattice. *Phys. Rev. Lett.* **110**, 076401 (2013).
- [34] Li, X., Zhao, E. & Liu, W. V. Topological states in a ladder-like optical lattice. *Nat. Commun.* **4**, 1523 (2013).
- [35] Zhang, W. & Zhai, H. Floquet topological states in shaking optical lattices. *Phys. Rev. A* **89**, 061603(R) (2014).
- [36] König, M. *et al.* The quantum spin Hall effect: theory and experiment. *J. Phys. Soc. Jpn.* **77**, 031007 (2008).
- [37] Liu, X.-J., Law, K. T. & Ng, T. K. Realization of 2D spin-orbit interaction and exotic topological orders in cold atoms. *Phys. Rev. Lett.* **112**, 086401 (2014).
- [38] Zhang, W. & Y, W. Topological Fulde-Ferrel-Larkin-Ovchinnikov states in spin-orbit coupled Fermi gases. *Nat. Commun.* **4**:2711 (2013).
- [39] Liu, X.-J. & Hu, H. Topological Fulde-Ferrell superfluids in spin-orbit-coupled atomic Fermi gases. *Phys. Rev. A* **88**, 023622 (2013).
- [40] Qu, C. *et al.* Topological superfluids with finite-momentum pairing and Majorana fermions. *Nat. Commun.* **4**:2710 (2013).
- [41] Chen, C. Inhomogeneous topological superfluidity in one-dimensional spin-orbit-coupled Fermi gases. *Phys. Rev. Lett.* **111**, 235302 (2013).
- [42] Pethick, C.J., & Smith, H. Bose-Einstein condensation in dilute gases. Cambridge university press, 2002.
- [43] Bijlsma, M., Heringa, B. A., & Stoof, H. T. D., *Phys. Rev. A* **61**, 053601 (2000).
- [44] Wu, C.J. & Das Sarma, S. $p_{x,y}$ -orbital counterpart of graphene: cold atoms in the honeycomb optical lattice. *Phys. Rev. B* **77**, 235107 (2008).
- [45] Ohashi, Y. & Griffin, A. BCS-BEC crossover in a gap of Fermi atoms with a Feshbach resonance. *Phys. Rev. Lett.* **89**, 130402 (2002).
- [46] Zhao, E. & Paramekanti, A. BCS-BEC crossover on the two-dimensional honeycomb lattice. *Phys. Rev. Lett.*, **97**, 230404 (2006).

Methods

Mean-field model in the momentum space. Consider the order parameter $\Delta(\mathbf{r}) = U\langle\psi_p\psi_s\rangle = \Delta e^{i\mathbf{Q}\cdot\mathbf{r}}$, where \mathbf{Q} is the pairing momentum, the thermodynamical potential is given by

$$\Omega = \frac{1}{2} \sum_{\mathbf{k}} \left(\epsilon_s(\mathbf{Q}/2 - \mathbf{k}) + \epsilon_p(\mathbf{Q}/2 - \mathbf{k}) \right) + \sum_{\mathbf{k}\lambda} \Theta(-E_\lambda(\mathbf{k})) E_\lambda(\mathbf{k}) + \frac{|\Delta|^2}{U}, \quad (6)$$

where $\Theta(x)$ is the Heaviside function representing the Fermi distribution at zero temperature. $E_\lambda(\mathbf{k})$ ($\lambda = 1, \dots, 4$) are the four eigenvalues of the BdG Hamiltonian $\mathcal{H}_{\text{BdG}}(\mathbf{k})$. The order parameter Δ and momentum \mathbf{Q} are hence given by self-consistently solving the saddle equations of the thermodynamical potential Ω :

$$\frac{\partial \Omega}{\partial \Delta} = 0, \quad \frac{\partial \Omega}{\partial \mathbf{Q}} = 0. \quad (7)$$

Mean-field model in the real space. In the real space the tight-binding Hamiltonian is written as

$$H_{\text{TB}} = H_0 + H_Z + H_\alpha + V_{\text{int}}, \quad (8)$$

where

$$H_0 = \sum_{\langle i,j \rangle} \left(-t_s c_i^\dagger c_j + t_p c_i^\dagger c_j \right) - \mu \sum_{i,\sigma=s,p} n_{i\sigma}, \quad (9)$$

$$H_Z = -h_z \sum_i (n_{is} - n_{ip}), \quad (10)$$

$$H_\alpha = \frac{\alpha}{2} \sum_i (c_{i-1p}^\dagger c_{is} - c_{i+1p}^\dagger c_{is} + \text{H.C.}), \quad (11)$$

$$V_{\text{int}} = -U \sum_i n_{is} n_{ip}, \quad (12)$$

The mean field order parameters

$$\Delta_i = U \langle c_{ip} c_{is} \rangle. \quad (13)$$

We have defined c_i and c_i^\dagger as the particle annihilation and creation operator on site i and the particle number operator $n_{i\sigma=s,p} = c_{i\sigma}^\dagger c_{i\sigma}$.

Mechanism of FFLO pairing. To demonstrate why the system favors FFLO pairing with a finite momentum

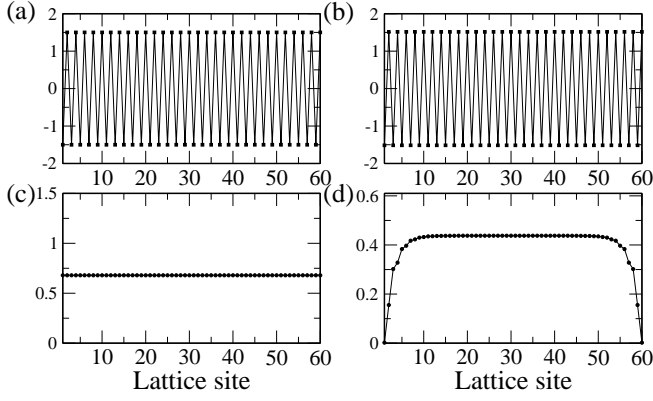


FIG. 5: **Self-consistently obtained order parameter in real space.** (a) $\Omega = 0.3t_s$, $\mu = 0.5t_s$, the system is in FFLO phase; (b) $\alpha = 0.3t_s$, $\mu = 0.5t_s$, the system is in FFLO phase; (c) $\alpha = 1.2t_s$, $\mu = 1.2t_s$, the system is in trivial BCS phase; (d) $\alpha = 1.2t_s$, $\mu = 1.2t_s$, $h = -0.5t_s$, the system is in topological BCS phase where we adopt open boundary condition for the appearance of MFs. Other parameters: $U = 4.0t_s$, $t_p = 3t_s$.

$Q = \pm\pi/a$ along the SOC direction, we start with the most simplest case, i.e., with vanishing α , h and μ and consider only the 1D system. If we choose the Nambu-Gorkov spinor $\Psi = (\psi_s(k_x), \psi_p(k'_x), \psi_p^\dagger(k'_x), \psi_s^\dagger(k_x))^T$, and introduce a general pairing order parameter $\Delta = U\langle\psi_p\psi_s\rangle$ the BdG Hamiltonian $\mathcal{H}_{\text{BdG}}(k_x)$ is rewritten as

$$\mathcal{H}_{\text{BdG}}(k_x, k'_x) = \begin{pmatrix} T(k_x, k'_x) & \Delta \\ \Delta^* & -\sigma_y T(k_x, k'_x) \sigma_y \end{pmatrix}, \quad (14)$$

where $T(k_x, k'_x) = \text{diag}[-t_s \cos(k_x a), t_p \cos(k'_x a)]$. When transferred to a new spinor basis $\Psi' = (\psi_s(k_x), \psi_p(-\frac{\pi}{a} + k'_x), \psi_p^\dagger(-\frac{\pi}{a} + k'_x), \psi_s^\dagger(k_x))^T$ through a unitary transformation $\Psi = U\Psi'$ with $U = \text{diag}(1, e^{i\pi x/a}, e^{i\pi x/a}, 1)$, we get

$$\begin{aligned} & \mathcal{H}'_{\text{BdG}}(k_x, k'_x) \mathcal{H}_{\text{BdG}}(k_x, k'_x) U \\ &= \begin{pmatrix} T(k_x, k'_x - \frac{\pi}{a}) & \Delta \\ \Delta^* & -\sigma_y T(k_x, k'_x - \frac{\pi}{a}) \sigma_y \end{pmatrix}. \end{aligned} \quad (15)$$

Notice that $T(k_x, k'_x - \frac{\pi}{a}) = \text{diag}[-t_s \cos(k_x a), -t_p \cos(k'_x a)]$ correspond to the conventional bands which are known to favor a BCS pairing in this new basis. It leads to $k_x = -(\pm\pi/a + k'_x)$ and hence $k_x + k'_x = \pm\pi/a$. As a result the pairing momentum should be fixed to $\pm\pi/a$.

Supplementary Information

Generation of on-site interactions. For a three dimensional optical lattice, each well can be expanded around its center as a harmonic oscillator potential

$$V(\mathbf{r}) = \frac{1}{2}m(\omega_x^2 x^2 + \omega_y^2 y^2 + \omega_z^2 z^2), \quad (16)$$

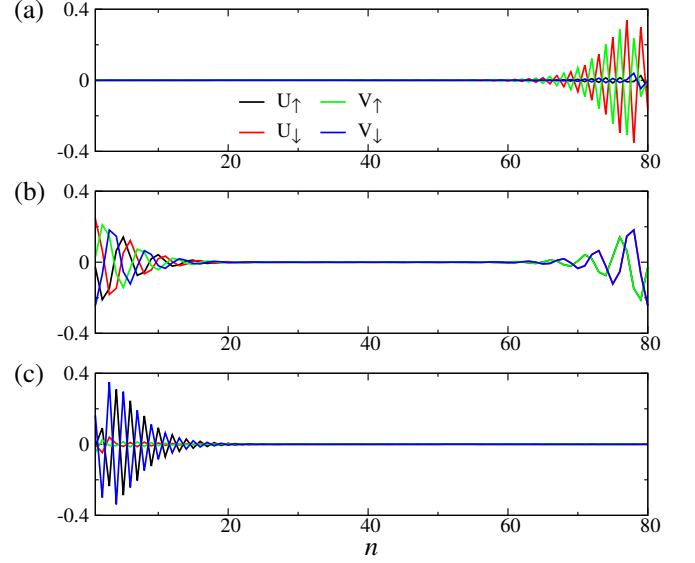


FIG. 6: **Wave functions of three pairs of edge states in real space.** (a,b,c) are the wave functions of the three pairs of sub-gap edge states as shown in Fig. 4 for energy level E_n where $n = 80, 160, 240$. (a,c) are the wave functions closely related to the topological insulator when there are no interactions; (b) are the wave functions of zero-energy Majorana fermions. Other parameters are $\alpha = 1.4t_s$, $\mu = -1.0t_s$, $h = 0.8t_s$, $U = 4.0t_s$.

where $\mathbf{r} = (x, y, z)$. We focus on the on-site interaction of the lowest two orbital states, for instance s - and p_x -orbital states, and assume an s -orbital state along both y - and z -axes. The wave functions for s - and p_x -orbital states in this harmonic potential are given by

$$\begin{aligned} \psi_s(\mathbf{r}) &= \left(\frac{m}{\pi\hbar}\right)^{\frac{3}{4}} \omega_x^{\frac{1}{4}} \omega_y^{\frac{1}{4}} \omega_z^{\frac{1}{4}} \\ &\times \exp\left[-\frac{m}{2\hbar}(\omega_x x^2 + \omega_y y^2 + \omega_z z^2)\right], \\ \psi_p(\mathbf{r}) &= \sqrt{2\pi} \left(\frac{m}{\pi\hbar}\right)^{\frac{5}{4}} \omega_x^{\frac{3}{4}} \omega_y^{\frac{1}{4}} \omega_z^{\frac{1}{4}} \\ &\times x \exp\left[-\frac{m}{2\hbar}(\omega_x x^2 + \omega_y y^2 + \omega_z z^2)\right]. \end{aligned} \quad (17)$$

In the Hartree-Fock approximation, the on-site interaction can be evaluated as,

$$\begin{aligned} -U &= \int d^3r_1 d^3r_2 V(\mathbf{r}_1 - \mathbf{r}_2) \left[|\psi_s(\mathbf{r}_1) \psi_p(\mathbf{r}_2)|^2 \right. \\ &\quad \left. - \psi_s^*(\mathbf{r}_1) \psi_p^*(\mathbf{r}_2) \psi_s(\mathbf{r}_2) \psi_p(\mathbf{r}_1) \right] \\ &= \frac{2m^4}{\pi^3 \hbar^4} \omega_x^2 \omega_y \omega_z \int d^3R d^3r V(\mathbf{r}) r_x (r_x/2 - R_x) \\ &\quad \times \exp\left[-\frac{m}{\hbar} \sum_{i=x,y,z} \omega_i (R_i^2 + r_i^2/4)\right], \end{aligned} \quad (18)$$

where we have introduced $\mathbf{r} = \mathbf{r}_1 - \mathbf{r}_2$ and $\mathbf{R} = (\mathbf{r}_1 + \mathbf{r}_2)/2$. For simplicity, we assume $\omega_y = \omega_z = \omega$ in fol-

lowing calculations. For the fermionic atomic gas with a dipole moment \mathbf{M} , the anisotropic interaction is expressed as

$$V(\mathbf{r}) = \frac{\mu_0 |\mathbf{M}|^2}{4\pi} \frac{[1 - 3(\hat{\mathbf{M}} \cdot \hat{\mathbf{r}})]^2}{r^3}, \quad (19)$$

where $\hat{\mathbf{M}} = \mathbf{M}/|\mathbf{M}|$ and $\hat{\mathbf{r}} = \mathbf{r}/|\mathbf{r}|$. Substituting it into the on-site interaction expression Eq. (18), we get

$$-U = 2 \left(\frac{m\omega}{\pi\hbar} \right)^{\frac{3}{2}} \frac{\mu_0 |\mathbf{M}|^2}{4\pi} \times F\left(\frac{\omega_x}{\omega}\right) \quad (20)$$

where

$$F\left(\frac{\omega_x}{\omega}\right) = \int_0^{2\pi} d\theta \int_0^\pi d\phi \frac{\left(\frac{\omega_x}{\omega}\right)^{\frac{3}{2}} \cos^2 \theta \sin^3 \phi [1 - 3(\hat{\mathbf{M}} \cdot \hat{\mathbf{r}})]^2}{\left(\frac{\omega_x}{\omega} \cos^2 \theta + \sin^2 \theta\right) \sin^2 \phi + \cos^2 \phi}.$$

In a real experiment, we can use fermionic atoms of ^{167}Er with $M = 7\mu_B$. The optical lattice can be created by laser beams with the wavelength $\lambda \approx 600\text{nm}$. The recoil energy of such an optical lattice is $E_R = \hbar^2/2m\lambda = 157nK$. For a typical tunneling energy $t_s \approx 0.36E_R \approx 55nK$. The on-site interaction $U \approx 224nK$ when $\omega_x/\omega \approx 0.3$ hence $U \approx 4t_s$ adopted in our paper can be obtained in real experiments.

Order parameters from self-consistent calculation in real space. Our numerical calculations are done in both momentum space and real space, which agrees very well with each other. In Fig. 5, we present the order parameter profiles in various phases from real space calculations.

Coexistence of edge states in the shaken optical lattice Without interaction, the system supports gap states which are localized on the system boundaries; When the interaction is turned on and the chemical potential cuts either the conduction or valence band, the system may support multiple edge states as shown in Fig. 6. The coexistence of the reminiscent edge states from topological insulator and the MFs edge states from topological superconductor may lead to many interesting transport properties in this system.

BCS-BEC crossover with two-photon coupling The interaction strength U can be easily tuned in cold atom experiments which provides a way to study the crossover from the BCS superfluids with weak attractive interaction to the Bose-Einstein condensation (BEC)

of strongly bounded molecules. BCS-BEC crossover has been widely studied in ultracold Fermi gases in various free space and optical lattice systems [45, 46]. In Fig. 7 we plot the phase diagrams in $h-U$ plane for a two-photon coupling process with different strengths of SOC (a) $\alpha = 0.7t_s$ (b) $\alpha = 1.4t_s$ for a certain value of chemical potential. In consistent with Fig. 3 (a)(b) we see FFLO superfluid phase dominates for small SOC and small Zeeman field, and BCS phase dominates for large Zeeman field or large SOC. The topological phase appears when

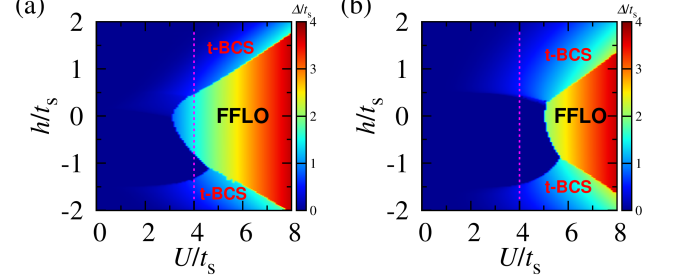


FIG. 7: **BCS-BEC crossover.** Color plots of the order parameter in the $h-U$ plane for small SOC (a) $\alpha = 0.7t_s$ and large SOC (b) $\alpha = 1.4t_s$. The chemical potential is taken as $\mu = -0.5t_s$, and $\Omega = 0.0$, $t_p = 3t_s$.

the strength of the Zeeman field exceeds a critical value for a medium value of interaction strength U and tends to disappear at the BEC side. Because SOC leads to an energy gap near half filling, the band insulator occupies a larger parameter region when SOC coupling strength is increased in the BCS side.

Spin 1/2 Fermi gas in a shaken optical lattice. We study the phase diagrams of a spin 1/2 (two internal states) Fermi gas in a shaken optical lattice, where atoms in one internal state only occupy the s -orbital band, and atoms in the other internal state occupy both s - and p -orbital band. In the shaking, the s - and p -orbital bands of the same species atoms are hybridized, and we only assume the interactions between different species in s - and p -orbital states. In the basis of $(\psi_{p\uparrow}(k_1), \psi_{s\uparrow}(k_1), \psi_{s\downarrow}(k_1), \psi_{s\downarrow}^\dagger(k_2), \psi_{s\uparrow}^\dagger(k_2), -\psi_{p\uparrow}^\dagger(k_2))^T$ with $k_1 = Q/2 + k_x$ and $k_2 = Q/2 - k_x$, the Hamiltonian in momentum space reads

$$\mathcal{H} = \begin{pmatrix} \varepsilon_{p\uparrow}(k_1) - h & \alpha \sin(k_1 a) & 0 & \Delta & 0 & 0 \\ \alpha \sin(k_1 a) & \varepsilon_{s\uparrow}(k_1) & 0 & 0 & 0 & 0 \\ 0 & 0 & \varepsilon_{s\downarrow}(k_1) & 0 & 0 & \Delta \\ \Delta & 0 & 0 & -\varepsilon_{s\downarrow}(k_2) & 0 & 0 \\ 0 & 0 & 0 & 0 & -\varepsilon_{s\uparrow}(k_2) & \alpha \sin(k_2 a) \\ 0 & 0 & \Delta & 0 & \alpha \sin(k_2 a) & -\varepsilon_{p\uparrow}(k_2) + h \end{pmatrix} \quad (21)$$

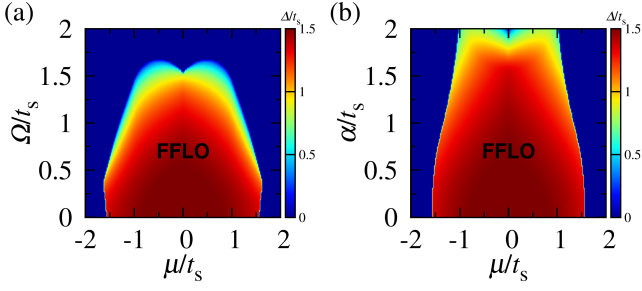


FIG. 8: **Phase diagram of the shaken optical lattice with the interaction with additional species of atoms** (a) one-photon coupling Ω or (b) two-photon coupling α . The color describes the magnitude of the order parameter Δ in unit of t_s . Other parameters $U = 4.0t_s$, $h = 0.0$, $t_p = 3t_s$.

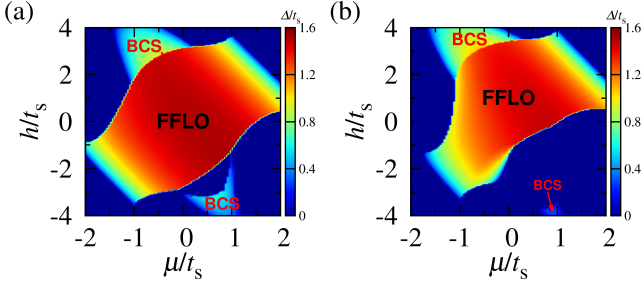


FIG. 9: **Effect of the Zeeman field on the phase diagram of the shaken optical lattice with the interaction with additional specie of atoms for a two-photon coupling.** (a) $\alpha = 0.7t_s$; (b) $\alpha = 1.4t_s$. We set $U = 4.0t_s$, $t_p = 3t_s$, $\Omega = 0.0$.

where $\varepsilon_{p\uparrow}(k_x) = t_p \cos(k_x a) - \mu$, $\varepsilon_{s\uparrow}(k_x) = -t_s \cos(k_x a) - \mu_{s\uparrow}$ and $\varepsilon_{s\downarrow}(k_x) = -t_s \cos(k_x a) - \mu$. For spin \uparrow in s -orbit states, we assume that it is full occupied with $\mu_{s\uparrow} = t_s$. Hence the interaction between the two different species in the same s -orbit states can be ignored. Fig. 8,9,10 demonstrate that similar phase diagrams are obtained where we identify the FFLO and BCS superfluids.

FFLO superfluids in a 2D shaken optical lat-

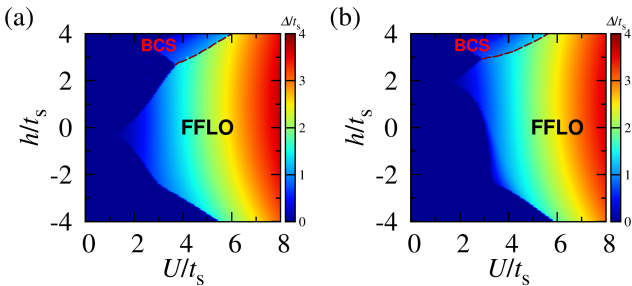


FIG. 10: **BCS-BEC crossover with the interaction with additional specie of atoms.** Color plots of the order parameter in the $h-U$ plane for smaller SOC (a) $\alpha = 0.7t_s$ and larger SOC (b) $\alpha = 1.4t_s$. The chemical potential is taken as $\mu = -0.5t_s$, and $\Omega = 0.0$, $t_p = 3t_s$.

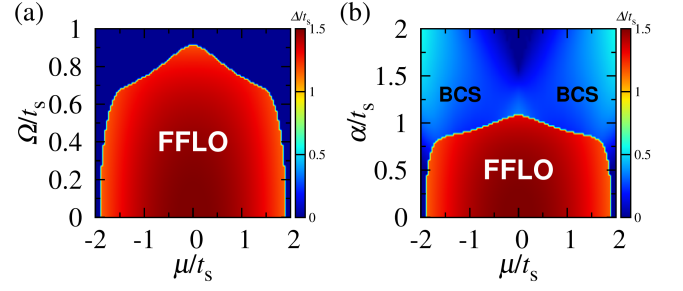


FIG. 11: **Phase diagram of the 2D shaken optical lattice with** (a) one-photon coupling Ω and (b) two-photon coupling α . The color describes the magnitude of the order parameter Δ in unit of t_s . Other parameters $U = 4.0t_s$, $h = 0.0$, $t_p = 3t_s$, $t_s^\perp = t_s$.

tice. The FFLO superfluids induced by the shaken optical lattice also exist in a 2D case. For simplicity, we consider the one-photon coupling Ω between the lowest two orbital states and assume the Cooper pairing can only have a nonzero momentum along x direction. In the basis of $(\psi_{p_x}(\mathbf{k}_1), \psi_s(\mathbf{k}_1), \psi_s^\dagger(\mathbf{k}_2), -\psi_{p_x}^\dagger(\mathbf{k}_2))^T$ with $\mathbf{k}_1 = (Q/2 + k_x, k_y)$ and $\mathbf{k}_2 = (Q/2 - k_x, -k_y)$, the Hamiltonian reads

$$\mathcal{H} = \begin{pmatrix} \varepsilon_{p_x}(\mathbf{k}_1) & \Omega & \Delta & 0 \\ \Omega & \varepsilon_s(\mathbf{k}_1) & 0 & \Delta \\ \Delta & 0 & -\varepsilon_s(\mathbf{k}_2) & \Omega \\ 0 & \Delta & \Omega & -\varepsilon_{p_x}(\mathbf{k}_2) \end{pmatrix} \quad (22)$$

where $\varepsilon_{p_x}(\mathbf{k}) = -t_p \cos(k_x a) + t_s^\perp \cos(k_y a) - \mu$ and $\varepsilon_s(\mathbf{k}) = t_s \cos(k_x a) + t_s^\perp \cos(k_y a) - \mu$. The phase diagram is shown in Fig. 11.